HBT High-Frequency Modeling and Integrated Parameter Extraction

Qian Cai, *Senior Member, IEEE,* Jason Gerber, *Member, IEEE,* Ulrich L. Rohde, *Senior Member, IEEE,* and Tom Daniel, *Member, IEEE*

***Abstract*— This paper presents, for the first time, a novel nonlinear model for accurate dc, small-signal, and noise characterization of AlGaAs–GaAs heterojunction bipolar transistors (HBT's). A new set of equations are introduced to take into account the bias, temperature, and frequency dependencies in noise calculations. This model provides significant improvement in predicting small-signal noise for HBT-based circuits. We also present an integrated method for accurate HBT model parameter extraction by fitting the dc, multibias s-parameter, and noise measurements simultaneously. The extracted model provides accurate small-signal, dc current, and noise characteristics. This technique is general and can be used for parameter extraction of other microwave devices such as MESFET's and high electron mobility transistors (HEMT's). Our new HBT model is validated using devices from different foundries. An integrated parameter extraction technique is demonstrated for a foundry HBT and excellent results are obtained.**

***Index Terms*— Heterojunction bipolar transistors, microwave devices, modeling, parameter estimation.**

I. Introduction

With the increasing demand of high speed and high signal-to-noise ratio (SNR) in analog and digital communication, high-frequency and low-noise circuits and systems are becoming more important. This leads to immense interest in the application of heterojunction bipolar transistors (HBT's) for high-speed digital and microwave circuits. HBT's, combining high transconductance, output resistance, and power density with high breakdown voltage [1], are rapidly becoming viable candidates for low-noise amplifier (LNA) applications across the entire microwave frequency spectrum and well into the millimeter bands. A particularly important application is in monolithic microwave integrated circuits (MMIC's) where highly accurate bias and temperature-dependent noise models are critical for first pass design success.

Accurate device models are critical to the success of the design of nonlinear microwave circuits such as amplifiers, oscillators, mixers, receivers and synthesizers [2]–[5], particularly in MMIC design [6]. Many HBT models have been developed during the last two decades using Monte Carlo methods [7], [8] and models based on the Gummel–Poon (GP) bipolar junction transistor (BJT) model [9], [10]. However, these models suffer from either computationally intensive or inadequate device performance prediction, especially in noise characterization.

Low-noise microwave circuit design engineers are often frustrated that the noise responses of the fabricated circuits are quite different from the results obtained using CAD programs. They may need several design passes to meet specifications. Even in mixer designs the noise of the fabricated circuits may be significantly higher than that predicted by the CAD tool. The discrepancy arises primarily from the poor estimation of the device noise figure.

Parameter extraction by fitting the model responses to measurements is the primary method to obtain the model parameter values of equivalent circuit models. Conventionally, parameter extraction is based on dc, s-parameter, and large-signal measurements (e.g., [11]–[13]). The models extracted are suitable for dc, small-signal, and large-signal analysis. However, noise analysis with these models often contains substantial errors.

In this paper, a novel HBT model for high-frequency and low-noise applications is presented. This model is based on a new formulation which takes into account the bias, temperature, and frequency dependencies of the device noise characteristics to provide accurate performance prediction. Two types of noise equivalent circuits, a linearized tee-model and a hybrid-π model, are derived from the modified GP model described in [14]–[17]. Self-heating effects are also taken into consideration using the thermal equivalent circuits.

We also present an integrated parameter extraction approach by fitting the model responses to the dc, multibias s-parameter, and multibias noise measurements simultaneously. The models extracted not only provide precise characterization of device small-signal and dc responses but also give accurate prediction of device noise performance. The models can be used in a variety of applications for small-signal and large-signal analysis as well as noise analysis. The advantages of our approach become more significant in the design of low-noise microwave circuits.

Our new HBT model is presented in Section II. The integrated parameter extraction technique is addressed in Sec-

Manuscript received March 31, 1997; revised August 15, 1997. This work was supported in part by the Air Force Phase II SBIR Program under Contract F33615-95-C-1707 on bias-dependent noise modeling of HBT's.

Q. Cai and J. Gerber are with Ansoft, Corporation, Compact Software Division, Elmwood Park, NJ 07407 USA.

U. L. Rohde is with Ansoft Corporation, Elmwood Park, NJ 07407 USA.

T. Daniel is with Lucent Technologies, Piscataway, NJ 08854 USA.

Publisher Item Identifier S 0018-9480(97)08351-8.

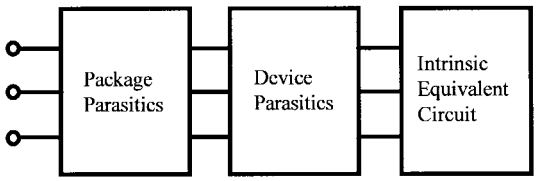

Fig. 1. Three parts of equivalent circuit for HBT model.

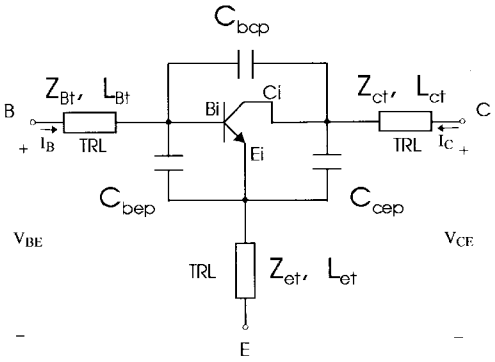

Fig. 2. A typical equivalent circuit representing package parasitics of HBT's.

tion III. HBT model validation using devices from various foundries is given in Section IV. Section V demonstrates the HBT model parameter extraction for a foundry device. Two models are extracted: Model 1 is based on dc and s-parameter measurements while Model 2 is based on dc, s-parameter, and noise measurements. Model 1 shows large errors in noise performance even though the dc and s-parameter fits are good. Model 2 provides accurate prediction in dc, s-parameter, and noise responses.

II. High-Frequency HBT Modeling

The equivalent circuits of our HBT model consists of three parts: intrinsic circuit, device parasitics, and package parasitics, as shown in Fig. 1. The device and package parasitics play a very important role in high-frequency modeling. Without considering these parasitics, the model would not be able to predict the ac performance accurately. A typical equivalent circuit representing package parasitics is shown in Fig. 2. The schematic of the intrinsic, extrinsic, and thermal circuits for our HBT model is depicted in Fig. 3. This circuit is a modified GP model implemented in SPICE [18]. The base resistor R_{bb} in the original GP model is split into R_{b1} and R_{b2} and a base capacitor C_{bx} is added between these two resistors. This modification is necessary for accurate HBT characterization at high frequencies. Additional base resistors and capacitors have been added to the model in [19] for the SPICE equivalent circuits. However, these components are external to the device and noise correlation is not able to be taken into account in SPICE simulators. In our paper, R_{b1}, R_{b2}, and C_{bx} are inside the device model incorporated into the harmonic balance simulator [20] which takes into account the noise correlation and provides a much more accurate noise prediction. The detailed dc, capacitance, and transient-time equations of the model are available in [20] which is derived from [10] and [15].

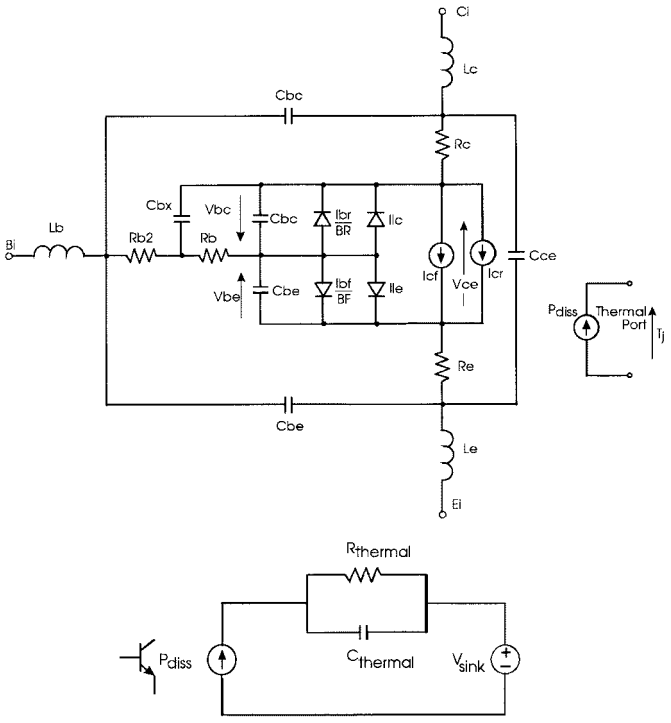

Fig. 3. Schematic of the intrinsic, extrinsic, and thermal circuits for the HBT model.

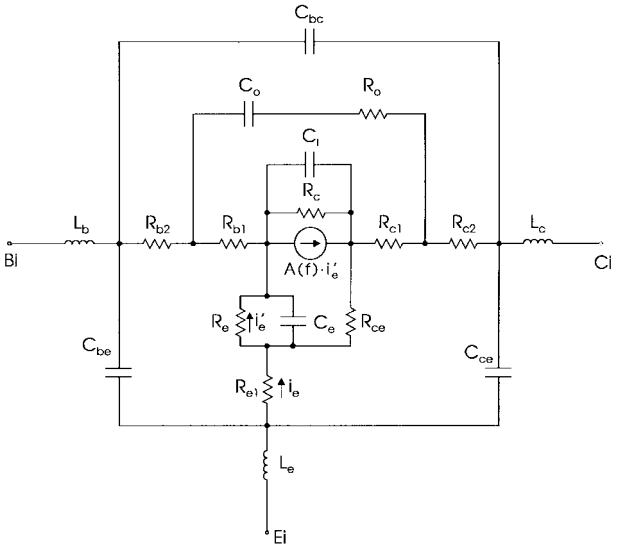

Fig. 4. The linearized T model for small-signal and noise calculations.

A. DC and Small-Signal Model

Using the intrinsic base–emitter voltage $V_{\rm be}$ and collector–emitter voltage $V_{\rm ce}$ shown in Fig. 3 as state variables, we can write the HBT model equations as

$$I_B = I_B(\phi, V_{\rm be}, V_{\rm ce}, T_j(\phi, V_{\rm be}, V_{\rm ce})) \quad (1a)$$

$$I_C = I_C(\phi, V_{\rm be}, V_{\rm ce}, T_j(\phi, V_{\rm be}, V_{\rm ce})) \quad (1b)$$

$$V_{\rm BE} = V_{\rm BE}(\phi, V_{\rm be}, V_{\rm ce}, T_j(\phi, V_{\rm be}, V_{\rm ce})) \quad (1c)$$

$$V_{\rm CE} = V_{\rm CE}(\phi, V_{\rm be}, V_{\rm ce}, T_j(\phi, V_{\rm be}, V_{\rm ce})) \quad (1d)$$

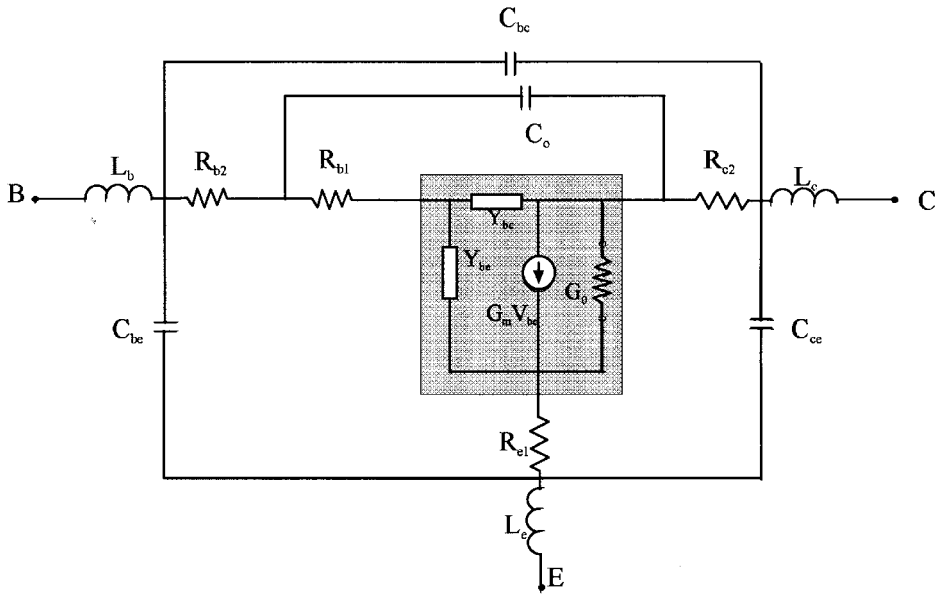

Fig. 5. The linearized hybrid-π model for small-signal and noise calculations.

which indicate that the extrinsic base current I_B, collector current I_C, base–emitter voltage $V_{\rm BE}$, and the collector–emitter voltage $V_{\rm CE}$, as shown in Fig. 2, are functions of model parameters ϕ, state variables $V_{\rm be}$ and $V_{\rm ce}$, and temperature T_j. The device temperature T_j is also dependent on the model parameters and state variables. Any two equations in (1) can be used to solve for the state variables. We use (1a) and (1d) with a Newton method in our dc simulation to obtain the dc operating points and produce constant I_B versus $V_{\rm CE}$ curves. For a fixed set of parameters ϕ, the Newton iteration is written as

$$\begin{bmatrix} V_{\rm be} \\ V_{\rm ce} \end{bmatrix}^{k+1} = \begin{bmatrix} V_{\rm be} \\ V_{\rm ce} \end{bmatrix}^{k} - \left(\begin{bmatrix} \frac{\partial I_B}{\partial V_{\rm bc}} & \frac{\partial V_{\rm CE}}{\partial V_{\rm bc}} \\ \frac{\partial I_B}{\partial V_{\rm ce}} & \frac{\partial V_{\rm CE}}{\partial V_{\rm ce}} \end{bmatrix}^{k} \right)^{-1} \times \begin{bmatrix} I_B - I_B^M \\ V_{\rm CE} - V_{\rm CE}^M \end{bmatrix}^{k} \tag{2}$$

where I_B^M and $V_{\rm CE}^M$ are the measured or applied base bias current and collector–emitter voltage. The entries to the Jacobian matrix can be obtained by derivating (1a) and (1d) w.r.t. the corresponding state variable, for instance,

$$\frac{\partial I_B}{\partial V_{\rm be}} = \frac{\partial I_B}{\partial V_{\rm be}} + \frac{\partial I_B}{\partial T_j} \frac{\partial T_j}{\partial V_{\rm be}}. \tag{3}$$

In our implementation, these entries are calculated analytically, which significantly reduces the computational time compared to the perturbation method used in other implementations (e.g. [10], [15]).

After the dc bias point is obtained, a small-signal equivalent circuit is then established by linearizing the model at the bias point and this is used for s-parameter and noise calculations. Two types of small-signal models are discussed in the following sections. As we will see, the bias, temperature, and frequency dependencies are taken into account in model evaluations for small-signal and noise simulation.

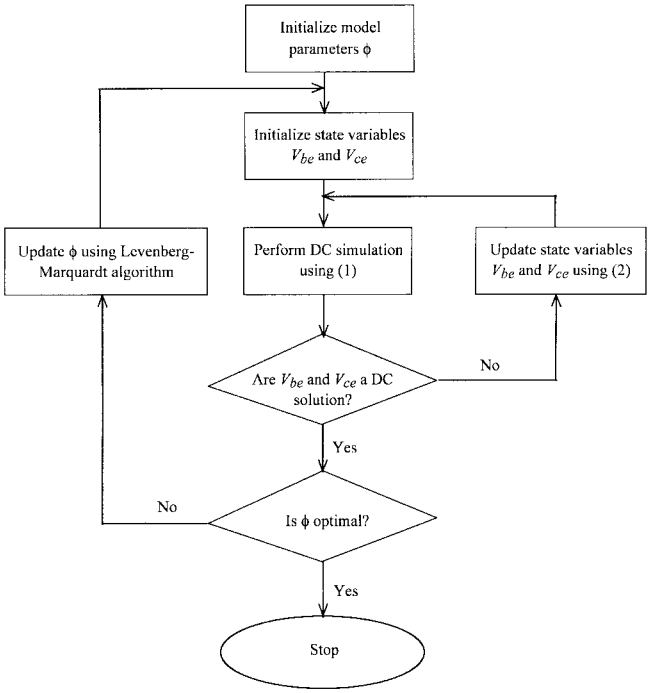

Fig. 6. Flowchart for model optimization.

B. Linearized T Model

The equivalent circuit for the linearized T model is sketched as Fig. 4. We add a collector–emitter resistor $R_{\rm ce}$ into the conventional T model [18] to provide more accurate device performance prediction. $R_{\rm ce}$ is also critical in parameter extraction for a good match between modeled and measured responses. The intrinsic linerized parameters A_0, C_i, R_C, R_e,

C_e, and $R_{\rm ce}$ are functions of ϕ, $V_{\rm be}$, $V_{\rm ce}$, and T_j obtained in the dc simulation. For example,

$$A_0 = A_0(\phi, V_{\rm be}, V_{\rm ce}, T_j(\phi, V_{\rm be}, V_{\rm ce})) = \left.\frac{\partial I_c'/\partial V_{\rm be}}{\partial I_b'/\partial V_{\rm be} + \partial I_c'/\partial V_{\rm be}}\right|_{\phi, V_{\rm be}, V_{\rm cc}, T_j = \text{constant}} \quad (4)$$

where

$$I_c' = I_{cf} - I_{cr}$$
$$I_b' = \frac{I_{bf}}{BF} + I_{le}.$$

I_{cf}, I_{cr}, I_{bf}, and I_{le} are illustrated in Fig. 3, and BF is the ideal forward current gain.

For the noise responses, the minimum noise figure $F_{\rm Min}$, the optimal noise reflection coefficient $\Gamma_{\rm opt}$, and the equivalent normalized noise resistance R_N are calculated using the following equations [16], [17].

$$F_{\rm Min} = a\frac{R_{b1} + R_{\rm opt}}{R_e} + \left(1 + \frac{f^2}{f_b^2}\right)\frac{1}{A_0} + \frac{F_C}{1+f}. \quad (5)$$

The optimum source resistance is calculated by

$$R_{\rm opt} = \left[R_{b1}^2 - X_{\rm opt}^2 + \left(1 + \frac{f^2}{f_b^2}\right)\frac{R_e(2R_{b1} + R_e)}{A_0 a}\right]^{1/2} \quad (6)$$

with the optimum source reactance

$$X_{\rm opt} = \left(1 + \frac{f^2}{f_b^2}\right)\frac{2\pi f C_e R_e^2}{A_0 a} \quad (7)$$

and the normalized noise resistance

$$R_N = R_{b1}\left(\alpha + 1 - \frac{1}{A_0}\right) + \frac{R_e}{2}\left\{\alpha + \frac{R_{b1}^2}{R_e^2}\left[1 - A_0 + \frac{f^2}{f_b^2} + \frac{f^2}{f_e^2} + \left(\frac{1}{A_0} - 1 - \frac{f^2}{f_b f_e}\right)^2\right]\right\} \quad (8)$$

where f is the operating frequency, f_b is the cutoff frequency of the ac common base current gain $A(f)$, A_0 is the dc current gain, and F_C is the Flicker noise corner frequency. The Flicker noise used for small-signal noise calculation is different from the one used for large-signal noise evaluation [20]. The coefficients α, a, and f_e are calculated as follows:

$$\alpha = \frac{1 + \left(\frac{f}{f_b}\right)^2}{A_0^2} \quad (9)$$

$$a = \left[\left(1 + \frac{f^2}{f_b^2}\right)\left(1 + \frac{f^2}{f_b^2}\right) - A_0\right]\frac{1}{A_0} \quad (10)$$

$$f_e = \frac{1}{2\pi N_{\rm fac} C_e R_e^2} \quad (11)$$

where $N_{\rm fac}$ is a noise factor.

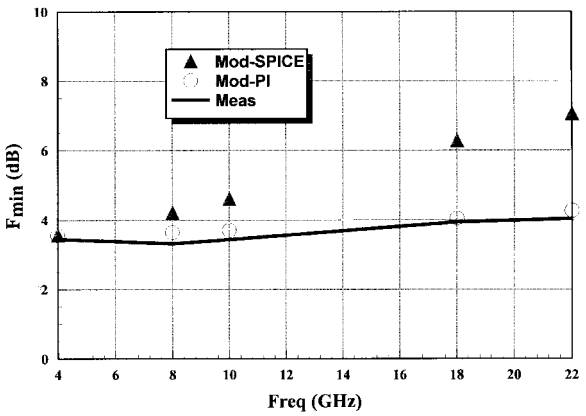

(a)

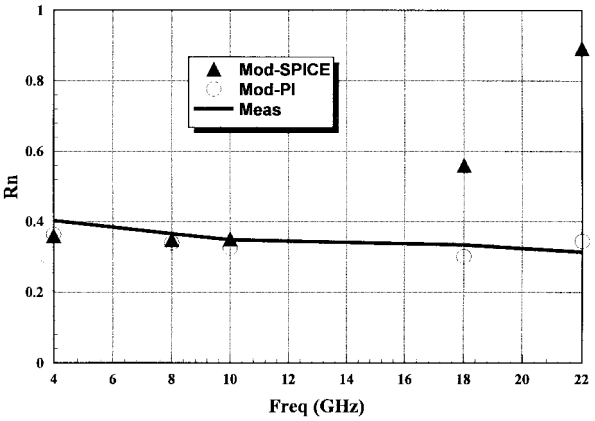

(b)

Fig. 7. Comparison of measured and modeled (our model and SPICE) noise parameters, (a) $F_{\rm Min}$ and (b) R_n, as a function of frequency for $V_{\rm CE} = 2.0$ V, $I_B = 428$ μA.

In addition to the above calculation, the effect of the device and package parasitic circuits are added to obtain the overall noise responses using a common two-port noise evaluation method.

C. Linearized Hybrid-π Model

The equivalent circuit for the linearized hybrid-π model is shown in Fig. 5. The intrinsic linerized parameters $Y_{\rm be}$, $Y_{\rm bc}$, G_{m0}, and G_0 are functions of model parameters ϕ, $V_{\rm be}$, $V_{\rm ce}$, and T_j obtained in the dc simulation. For example,

$$G_{m0} = G_{m0}(\phi, V_{\rm be}, V_{\rm ce}, T_j(\phi, V_{\rm be}, V_{\rm ce})) = \left.\frac{\partial I_c'}{\partial V_{\rm be}}\right|_{\phi, V_{\rm be}, V_{\rm cc}, T_j = \text{constant}}. \quad (12)$$

The intrinsic noise model of this hybrid-π circuit is developed by incorporating the correlation of the noise sources and the frequency dependency of the noise sources. The normalized noise correlation matrix can be written as

$$C = \frac{1}{4KT_jB}\begin{bmatrix} \overline{i_b i_b^*} & \overline{i_b i_c^*} \\ \overline{i_c i_b^*} & \overline{i_c i_c^*} \end{bmatrix} \quad (13)$$

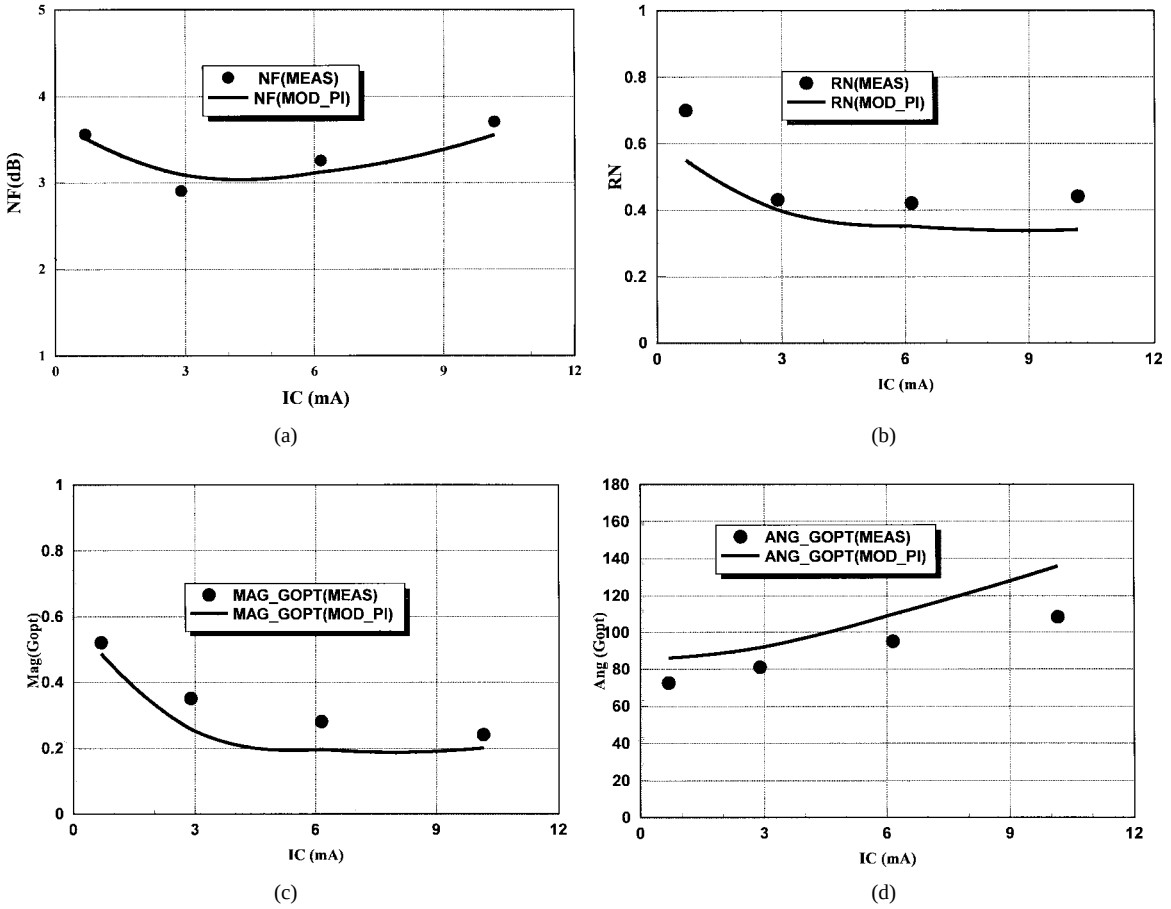

Fig. 8. Bias dependency of the noise parameters versus collector current at 10 GHz, biased at $V_{\rm CE} = 2$ V and I_B varied from 50 to 200 μA: (a) N_F, (b) R_N, (c) $|\Gamma_{\rm opt}|$, and (d) $\angle\Gamma_{\rm opt}$.

where

$$\overline{i_b i_b^*} = 4KT_j \,\mathrm{Re}[Y_{11}]B - 2qI_bB \tag{14a}$$

$$\overline{i_c i_b^*} = 2KT_j(G_m - 2\,\mathrm{Re}[Y_{12}])B - 2qI_cB \tag{14b}$$

$$\overline{i_c i_c^*} = 4KT_j \,\mathrm{Re}[Y_{22}]B + 2qI_cB \tag{14c}$$

where K is the Boltzmann constant, B is the bandwidth, q is the electron charge, I_b and I_c are the intrinsic base and collector currents, respectively, Y_{11}, Y_{12}, Y_{22} correspond to the intrinsic Y matrix of the intrinsic model as shown in Fig. 5 (shaded region), and $\mathrm{Re}[Y_{ij}]$ represents the real part of Y_{ij}.

At zero frequency (dc), the noise power terms $\overline{i_b i_b^*}$ and $\overline{i_c i_c^*}$ of the intrinsic device reduce to the SPICE shot noise model. Also, the cross-correlation terms reduce to zero indicating that there is no noise component common to both the collector and base currents.

The intrinsic noise parameters $(R_N, F_{\rm Min}, \Gamma_{\rm opt})$ are derived from the correlation matrix C of (13) as

$$R_N = C_{11} \tag{15}$$

$$G_{\rm opt} = \sqrt{\frac{C_{22}}{C_{11}} - \left[\frac{\mathrm{Im}(C_{12})}{C_{11}}\right]^2} \tag{16}$$

$$B_{\rm opt} = \frac{\mathrm{Im}(C_{12})}{C_{11}} \tag{17}$$

$$F_{\rm Min} = 1 + 2\sqrt{C_{11}C_{22} - \mathrm{Im}(C_{12})^2} + \mathrm{Re}(C_{12}) \tag{18}$$

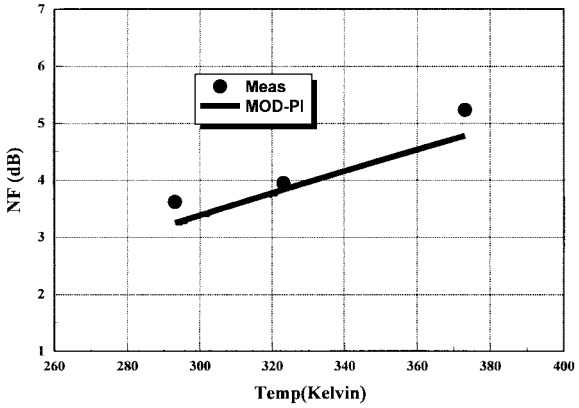

Fig. 9. Temperature dependency of the noise figure at 10 GHz, biased at $V_{\rm CE} = 1$ V and $I_B = 100$ μA. Temperature was varied from 20 °C to 100 °C.

where $\mathrm{Re}(C_{12})$ and $\mathrm{Im}(C_{12})$ are the real part and imaginary part of C_{12}, respectively.

III. Integrated Parameter Extraction

In this section, we present integrated parameter extraction by fitting the dc, multibias s-parameter, and noise measurements simultaneously.

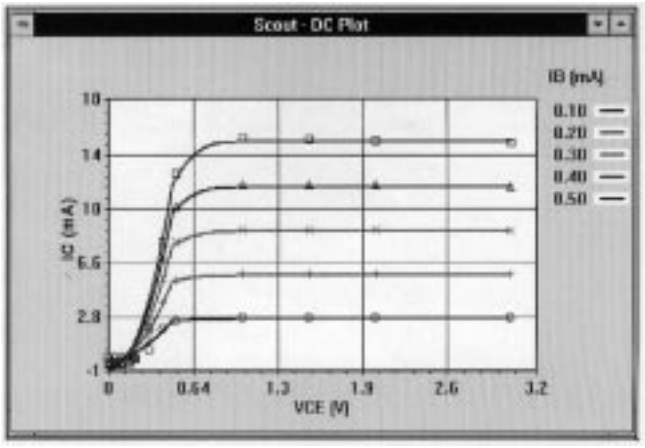

(a)

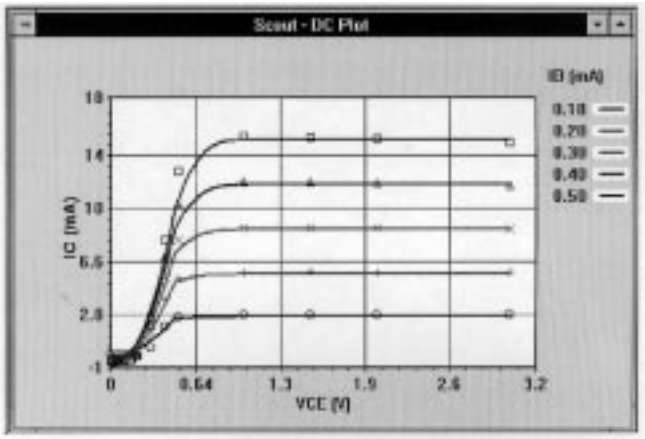

(b)

Fig. 10. Measured (discrete points) and modeled (solid lines) dc I–V curves of (a) Model 1 and (b) Model 2.

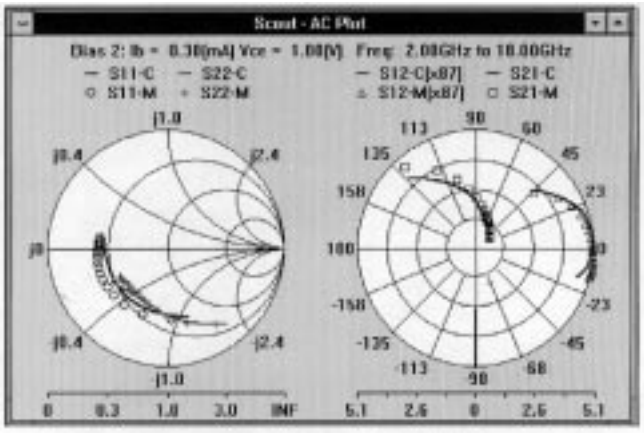

(a)

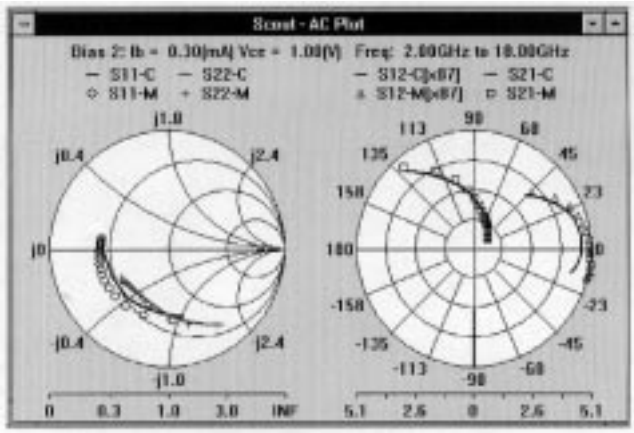

(b)

Fig. 11. Measured (discrete points) and modeled (solid lines) S parameters of (a) Model 1 and (b) Model 2 at bias point $I_B = 0.3$ mA and $V_{\rm CE} = 1$ V.

A. Formulation of Integrated Parameter Extraction

The objective function for optimization in our integrated parameter extraction include dc, s-parameter, and noise measurements. It is formulated as

$$E_{\rm total}(\phi) = E_{\rm DC}(\phi) + E_S(\phi) + E_N(\phi) \tag{19}$$

where ϕ's are the model parameters to be extracted, $E_{\rm total}$ is the total error, and

$$E_{\rm DC}(\phi) = \sum_{i=1}^{N_{\rm DC}} \sum_{k,l}^{N_P} ||W_{{\rm DC}_{ikl}}[R_{{\rm DC}_{ikl}}(\phi) - M_{{\rm DC}_{ikl}}]|| \tag{20a}$$

$$E_S(\phi) = \sum_{i=1}^{N_{\rm SDC}} \sum_{j=1}^{N_{\rm SF}} \sum_{k,l}^{N_P} ||W_{S_{ijkl}}[R_{S_{ijkl}}(\phi) - M_{S_{ijkl}}]|| \tag{20b}$$

$$E_N(\phi) = \sum_{i=1}^{N_{\rm NDC}} \sum_{j=1}^{N_{\rm NF}} \sum_{k}^{N_{\rm NP}} ||W_{N_{ijk}}[R_{N_{ijk}}(\phi) - M_{N_{ijk}}]|| \tag{20c}$$

are the dc error, s-parameter error, and noise error, respectively. N_P is the number of ports of the device. $N_{\rm DC}$ is the number of dc measurement points. $N_{\rm SDC}$ and $N_{\rm SF}$ are, respectively, the number of bias points and frequencies at which the s-parameter measurements are taken. $N_{\rm NP}$ is the number of noise parameters and $N_{\rm NDC}$ and $N_{\rm NF}$ are, respectively, the number of bias points and frequencies at which the noise measurements are taken. The R's and M's are the model responses and the corresponding measurements. The W's are the weighting factors applied to the corresponding errors. The $||\bullet||$ denotes the least-squares norm. A Levenberg–Marquardt optimization process was applied to

$$\underset{\phi}{\text{minimize}}\ E_{\rm total}(\phi). \tag{21}$$

The dc, multibias s-parameter, and multibias noise measurements are simultaneously matched to the model responses during optimization. A direct parameter extraction and systematic optimization strategy [21] can be used for efficient model extraction.

B. Model Optimization

The optimization scheme consists of two iteration loops. The first iteration loop is for dc simulation to obtain the dc

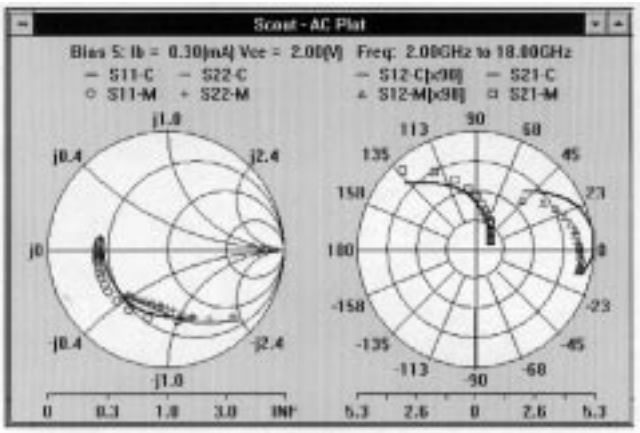

(a)

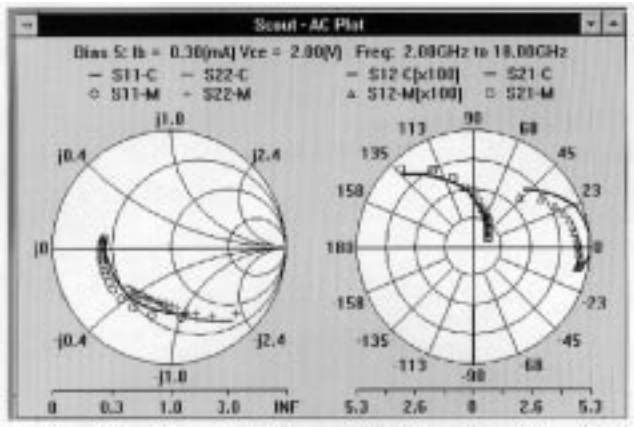

(b)

Fig. 12. Measured (discrete points) and modeled (solid lines) S parameters of (a) Model 1 and (b) Model 2 at bias point $I_B = 0.3$ mA and $V_{\rm CE} = 2$ V.

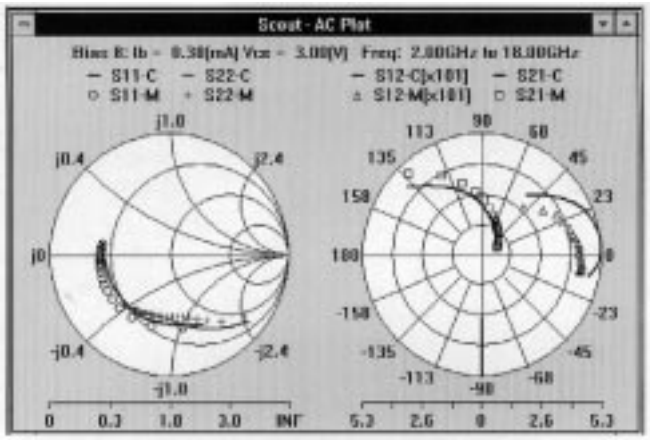

(a)

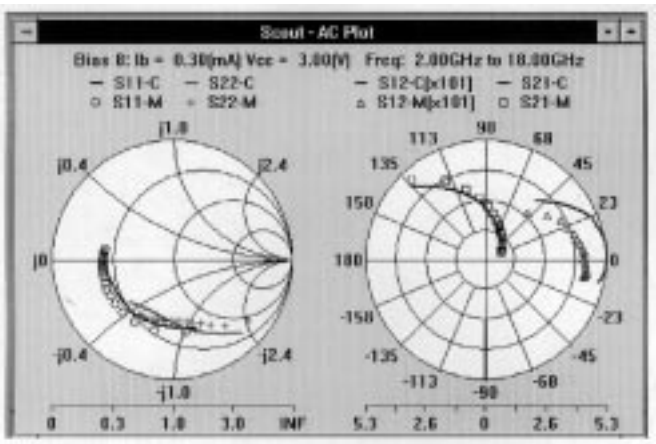

(b)

Fig. 13. Measured (discrete points) and modeled (solid lines) S parameters of (a) Model 1 and (b) Model 2 at bias point $I_B = 0.3$ mA and $V_{\rm CE} = 3$ V.

operation point as described in Section II. The second loop is used for adjusting the model parameters ϕ to match the model responses to the measurements. This procedure can be described by the following algorithm.

Step 1: Initialize the model parameter ϕ.

Step 2: Initialize the state variables $V_{\rm be}$ and $V_{\rm ce}$.

Step 3: Perform a dc simulation at each bias point to obtain the solution for state variables using the Newton iteration of (2).

Step 4: Obtain the linearized small-signal circuit and calculate the model responses including the s parameters and noise parameters at each bias point and frequency.

Step 5: Calculate the objective function for optimization using (19) and (20).

Step 6: If ϕ is optimal, stop. Otherwise, update ϕ according to the Levenberg-Marquardt optimization algorithm and go to Step 2.

This algorithm is illustrated by the flowchart in Fig. 6.

IV. Noise Model Validation

We use the linearized hybrid-π model for noise model validation in this section and leave the linearized T model for integrated parameter extraction example which will be discussed in Section V.

To validate the model, on-wafer bias and temperature-dependent noise parameter measurements are performed using the ATN-NP5 system for various foundries. Parameter extraction is performed using the procedure and model described above.

Fig. 7 compares the measured and modeled noise parameters for a foundry HBT biased at $V_{\rm CE} = 2$ V and $I_B = 428$ μA. Two models are compared with the measured result; our model, referred to as *'Mod_PI'* and the SPICE shot noise model (referred as *'MOD_SPICE'*), used in SPICE and harmonic balance simulators. From the results, it is evident that at lower frequencies both models predict the same, however, for reasons as explained earlier, at higher frequencies the SPICE noise model deviates rapidly from the measurements while our model is very consistent with the measurements.

The next validation process is the model's accuracy with bias. For this case, the base current is varied from 50 to 200 μA, and $V_{\rm CE}$ is set to 2 V. The frequency is 10 GHz. Fig. 8 illustrates the bias-dependent noise characteristics for a foundry HBT. Very good correlation is obtained between the measured and modeled noise parameters.

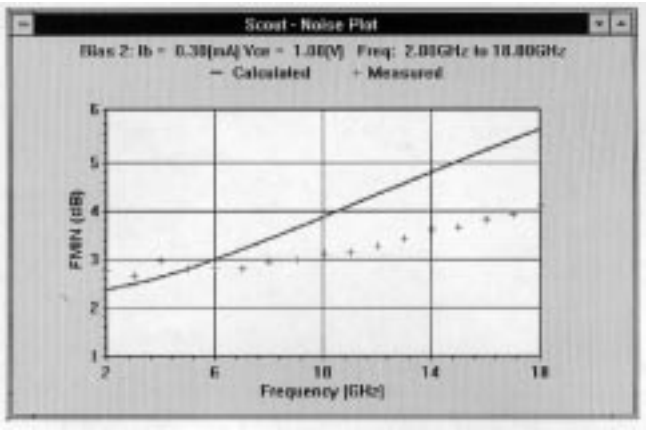

(a)

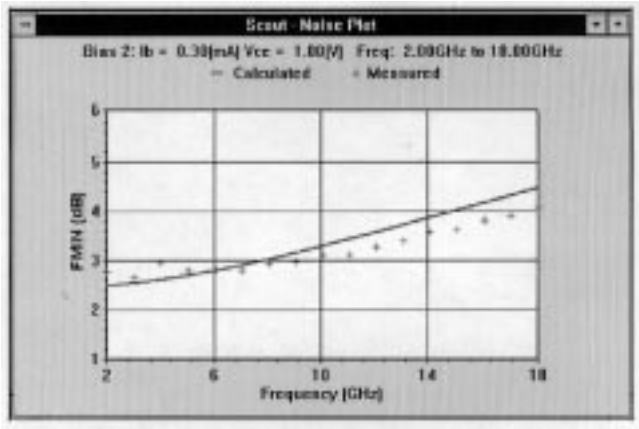

(b)

Fig. 14. Measured (discrete points) and modeled (solid lines) minimum noise figures of (a) Model 1 and (b) Model 2 at bias point $I_B = 0.3$ mA and $V_{\rm CE} = 1$ V.

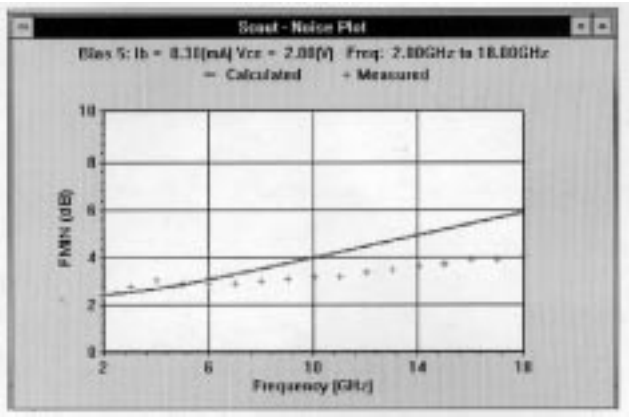

(a)

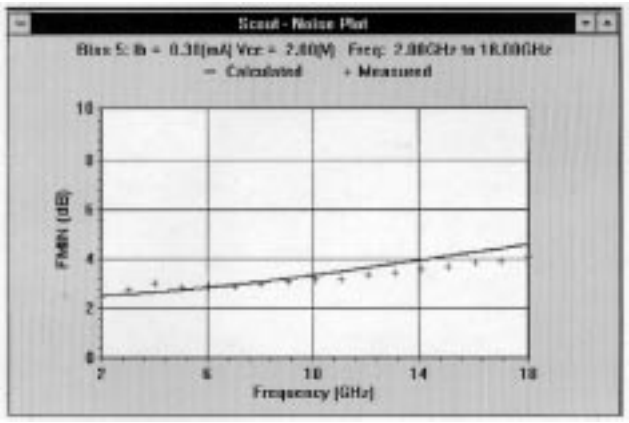

(b)

Fig. 15. Measured (discrete points) and modeled (solid lines) minimum noise figures of (a) Model 1 and (b) Model 2 at bias point $I_B = 0.3$ mA and $V_{\rm CE} = 2$ V.

Finally, the temperature-dependent model is validated as shown in Fig. 9. The noise figure of the HBT is plotted versus temperature in Kelvins. In this case, the device is biased at $V_{\rm CE} = 1$ V and $I_B = 100$ μA and the temperature varied from 293 °K to 373 °K (20 °C to 100 °C). We can see a very good match between the measured and modeled results.

V. Parameter Extraction of an HBT Model

Parameter extraction of an HBT model is carried out using the linearized T model illustrated in Section II.

The data used for parameter extraction include dc measurements at 60 points, and s-parameter measurements and noise measurements at 9 bias points and 17 frequencies. Two models are extracted: Model 1 using dc and s-parameter measurements while Model 2 using dc, s-parameter, and noise measurements. The modeled and measured dc responses are plotted in Fig. 10. The modeled and measured S parameters at three bias points are shown in Figs. 11–13. The modeled and measured minimum noise figures at three bias points are shown in Figs. 14–16. From Figs. 10–13, we can see that the dc responses and S parameters of both models match the measurements very well. However, the noise responses of Model 2 are much closer to the measurements than those of Model 1 which are illustrated in Figs. 14–16. If both models are used for noise analysis in circuit design, Model 2 will provide much more accurate results than Model 1.

VI. Conclusion

We have presented a novel nonlinear model for accurate dc, small-signal, and noise characterization of AlGaAs–GaAs HBT's. Two linearized model topologies have been described. Our model takes into account the bias, temperature, and frequency dependencies for small-signal and noise calculations and provides accurate device performance prediction. The model has been validated using devices from different foundries. This model can be implemented into SPICE or harmonic balance simulators thereby facilitating the design of microwave integrated circuits which incorporate HBT's. Our novel innovative noise calculation method can be similarly applied to the noise calculations of the FET device family.

We have exploited an integrated parameter extraction method fitting dc, multibias s-parameter, and multibias noise measurements simultaneously. The models extracted using this approach are capable of predicting the device small-signal responses and dc characteristics as well as noise performances accurately and can be used in a wide range of applications. Microwave circuit design engineers will benefit from such

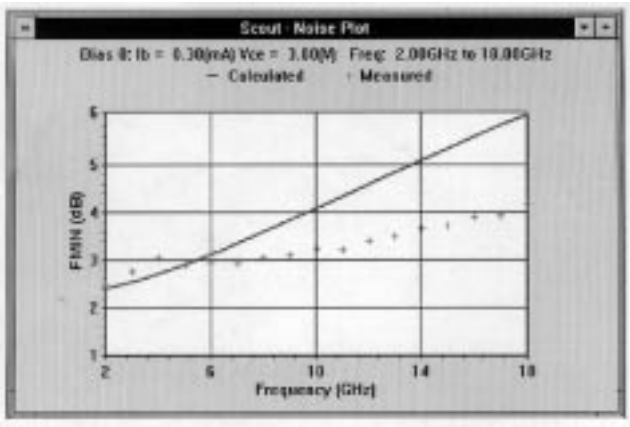

(a)

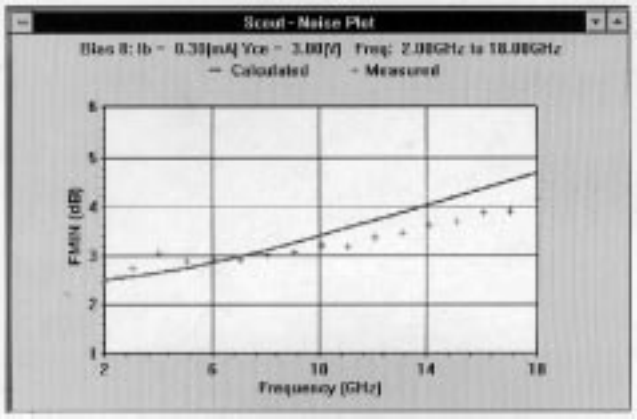

(b)

Fig. 16. Measured (discrete points) and modeled (solid lines) minimum noise figures of (a) Model 1 and (b) Model 2 at bias point $I_B = 0.3$ mA and $V_{\rm CE} = 3$ V.

models to attain first-pass circuit design and thus reduce the development cost. This creative technique is general and can be used for parameter extraction of other devices.

ACKNOWLEDGMENT

The authors gratefully acknowledge discussions with Dr. R. Pucel. The authors would like to thank R. Neidhard of WL/ELM, Wright Patterson Air Force Base for providing measurements. Participation of the two foundries toward model validation is greatly appreciated.

REFERENCES

[1] R. Anholt, *Electrical and Thermal Characterization of MESFET's, HEMT's, and HBTs*. Norwood, MA: Artech, 1995.
[2] G. Vendelin, A. M. Pavio, and U. L. Rohde, *Microwave Circuit Design Using Linear and Nonlinear Techniques*. New York: Wiley, 1990.
[3] E. L. Kollberg, Ed., *Microwave and Millimeter-Wave Mixers*. Piscataway, NJ: IEEE Press, 1984.
[4] U. L. Rohde, J. Whitaker, and T. N. N. Bucher, *Communications Receivers*, 2nd ed. New York: McGraw-Hill, 1997.
[5] U. L. Rohde, *Microwave and Wireless Synthesizers: Theory and Design*. New York: Wiley, 1997.
[6] R. A. Pucel, Ed., *Monolithic Microwave Integrated Circuits*. Piscataway, NJ: IEEE Press, 1985.
[7] K. Tomizawa, Y. Awano, and N. Hashizume, "Monte Carlo simulation of AlGaAs/GaAs heterojunction bipolar transistors," *IEEE Electron Device Lett.*, vol. EDL-5, p. 362, 1984.
[8] J. Hu, K. Tomizawa, and D. Pavlidis, "Monte Carlo approach to transient analysis of HBT's with different collector designs," *IEEE Electron Device Lett.*, vol. 10, pp. 55–57, 1989.
[9] A. A. Grinberg, M. Shur, R. Fisher, and H. Morkoc, "Investigation of the effects of graded layer and tunneling on the performance of AlGaAs/GaAs heterojunction bipolar transistors," *IEEE Trans. Electron Devices*, vol. ED-31, pp. 1758–1765, 1984.
[10] R. Anholt, J. Gerber, R. Tayrani, and J. Pence, "HBT model parameter extractor for SPICE and harmonic balance simulators," in *IEEE MTT-S Int. Microwave Symp. Digest*, 1994, pp. 1257–1260.
[11] J. W. Bandler, R. M. Biernacki, Q. Cai, S. H. Chen, S. Ye, and Q. J. Zhang, "Integrated physics-oriented statistical modeling, simulation and optimization," *IEEE Trans. Microwave Theory Tech.*, vol. 40, pp. 1374–1400, 1992.
[12] S. G. Skaggs, J. Gerber, G. Bilbro, and M. B. Steer, "Parameter extraction of microwave transistors using a hybrid gradient descent and tree annealing approach," *IEEE Trans. Microwave Theory Tech.*, vol. 41, pp. 726–729, 1993.
[13] T. Fernández, Y. Newport, J. M. Zamanillo, A. Tazón, and A. Mediavilla, "Extracting a bias-dependent large-signal MESFET model from pulsed I/V measurements," *IEEE Trans. Microwave Theory Tech.*, vol. 44, pp. 372–378, 1996.
[14] M. E. Hafizi, C. R. Crowell, and M. E. Grupen, "The DC characteristics of AlGaAs/GaAs heterojunction bipolar transistors with application to device modeling," *IEEE Trans. Electron Devices*, vol. ED-37, pp. 2121–2129, 1990.
[15] R. Anholt, J. Gerber, R. Tayrani, and J. Pence, "A self-heating HBT model for harmonic balance simulators with parameter extraction," *1994 Asia-Pacific Microwave Conf.*, 1994, pp. 1029–1032.
[16] U. L. Rohde and C. R. Chang, "Parameter extraction for large-signal noise models and simulation of noise in large-signal circuits," *Microwave Journal*, pp. 222–239, May 1993.
[17] R. A. Pucel and U. L. Rohde, "An accurate expression for the noise resistance R_n of a bipolar transistor for use with the Hawkins noise model," *IEEE Microwave and Guided Wave Letters*, vol. 3, pp. 35–37, 1993.
[18] *Semiconductor Modeling with SPICE*, P. Antognetti and G. Massobrio (Eds.), NY: McGraw-Hill, New York, 1988.
[19] *Communications Components Designer's Catalog, GaAs and Silicon Products*, Hewlett Packard Data Book, 1993.
[20] *Microwave Harmonica Reference Manual*, Ansoft Corporation/Compact Software Division, Elmwood Park, NJ.
[21] *Compact Scout Reference Manual*, Ansoft Corporation/Compact Software Division, Elmwood Park, NJ.

Qian Cai (S'90–M'92–SM'95) was born in Zhanjiang, Guangdong, China, on October 16, 1957. He received the M.S.(Eng.) degree from the South China University of Technology, Guangzhou, China, in 1986 and the Ph.D. degree from McMaster University, Hamilton, ON, Canada, in 1992.

From June 1982 to July 1983, he was an Instrumentation Engineer in the Guangdong Petrochemical Construction Company, Guangzhou, China. He was an Assistant Lecturer from June 1986 to June 1988, and a Lecturer from July 1988 to August 1988, in the Department of Electrical Engineering, Guangdong University of Technology, Guangzhou, China. He was awarded a Chinese Government Graduate Scholarship and joined the Simulation Optimization Systems Research Laboratory and the Department of Electrical and Computer Engineering, McMaster University, in September 1988. He held a Clifton W. Sherman Graduate Scholarship for the academic year 1990–1991. He was a Post-Doctoral Fellow from June 1992 to May 1993 and a Research Associate from June 1993 to November 1993 in the Department of Electrical and Computer Engineering, McMaster University. He was awarded an Industrial Research Fellowship from the Natural Sciences and Engineering Research Council of Canada for 1993 to 1995 and joined Optimization Systems Associates, Inc., Dundas, ON, Canada, where he was a Research Engineer from December 1993 to September 1995. He joined Compact Software, Inc. (now Compact Software Division, Ansoft Corporation), Elmwood Park, NJ, as a Senior Microwave Circuit Engineer in October 1995. His professional interests include circuit CAD, device physics and modeling, simulation and optimization, statistical modeling and design, sensitivity analysis and yield optimization.

Jason Gerber (S'85–M'88) received the B.S.E.E. degree from Drexel University, Philadelphia, PA, in 1986 and the M.S.E.E. degree from the University of Massachusetts, Amherst, in 1989.

He joined Compact Software (now Compact Software Division, Ansoft Corporation), Elmwood Park, NJ, in 1988, developing nonlinear harmonic-balance simulation tools and transistor parameter extration tools. Since 1994, he has been managing the microwave engineering group, overseeing the development of circuit analysis tools. His interests are in the research and development of high-frequency circuit analysis, transistor characterization, and the development of integrated design tools.

Ulrich L. Rohde (M'74–SM'74) studied electrical engineering and radio communications at the University of Munich and Darmstadt, Germany. He received the Ph.D. degree in electrical engineering in 1978 and the Sc.D. degree (with honors) in radio communications in 1979.

He is President of Communications Consulting Corporation, Executive Vice President of Ansoft Corporation for Strategic Planning, Pittsburg, PA, Chairman of Synergy Microwave Corporation, Paterson, NJ, and partner of Rohde & Schwarz, Munich, West Germany, a multinational company specializing in advanced test and radio communications systems. Previously, he was the President of Compact Software, Inc., Paterson, NJ, and Business Area Director for Radio Systems of RCA, Government Systems Division, Camden, NJ, responsible for implementing communications approaches for military secure and adaptive communications. In May 1997, he was appointed Associate Professor of Electrical Engineering at the University of Oradea, Romania. From 1990 to 1992, he was appointed Visiting Research Professor at the New Jersey Institute of Technology, Department of Electrical Engineering, Newark, NJ. He has also been a member of the staff at George Washington University, Washington, DC, since 1982 and an Adjunct Professor in the Electrical Engineering and Computer Sciences departments of the same university, where he gave numerous lectures worldwide regarding communication theory and digital frequency synthesizers. In addition, as a Professor of Electrical Engineering at the University of Florida, Gainesville, since 1977, he taught a radio communications course. He has published more than 60 scientific papers in professional journals, as well as six books: *Microwave and Wireless Synthesizers: Theory and Design* (New York: Wiley, 1997), *Communications Receivers*, (New York, McGraw-Hill, 1997, 2nd ed., with co-authors Jerry Whitaker and T. N. N. Bucher), *Microwave Circuit Design Using Linear and Nonlinear Techniques* (New York: Wiley, 1990, with co-authors George Vendelin and Anthony M. Pavio), *Communications Receivers: Principles and Design* (New York: McGraw-Hill, 1987), *Digital PLL Frequency Synthesizers: Theory and Design* (Englewood Cliffs, NJ: Prentice-Hall, 1983), and *Transistoren bei hoechsten Frequenzen* (1965, in German).

Dr. Rohde is a member of Eta Kappa Nu, Executive Association of the Graduate School of Business—Columbia University, New York, the Armed Forces Communications & Electronics Association, a fellow of the Radio Club of America, and a life member of the Amateur Radio Relay League. He holds an Extra Class U.S. amateur license and is an ARRL-accredited VE. He also holds the FCC General Radiotelephone Operator License, a Global Maritime Distress and Safety System maintainer license, both with radar endorsements, and a second-class Radiotelegraph operator license.

Tom Daniel (S'92–M'95) received the B.E. degree in electronics and communication engineering from Mangalore University, India, in 1989 and the M.S. degree in electrical engineering from Drexel University, Philadelphia, PA, in 1992.

From 1989 through 1992, he worked as a Research Assistant at the Center for Microwave and Lightwave Engineering, Drexel University. From 1992 to 1997, he worked for Compact Software as a Senior Microwave Engineer. Currently, he is with the Global Wireless Products Group of Lucent Technologies, working in the areas of RFIC design and system analysis on CDMA/AMPS-based handsets for wireless applications.